2012 American Control Conference
Fairmont Queen Elizabeth, Montréal, Canada
June 27-June 29, 2012

Adaptive Forward-Propagating Input Reconstruction for Nonminimum-Phase Systems

Anthony M. D'Amato and Dennis S. Bernstein

Abstract— **Input reconstruction is a process where the inputs to a system are estimated using the measured system output, and possibly some modeling information from the system model. One way to achieve this goal is to invert the system model and cascade delays to guarantee that the inverse is proper. A standing issue in input reconstruction lies in the inversion of nonminimum-phase systems, since the inverse model is unstable. We consider two methods for achieving input reconstruction despite the presence of nonminimum-phase zeros. First, we develop an open-loop partial inversion of the system model using a finite number of frequency points, where the partial inverse is a finite impulse response model and therefore is guaranteed to be asymptotically stable. Second, we examine a closed-loop approach that uses an infinite impulse response model. We demonstrate both methods on several illustrative examples.**

I. Introduction

Unlike state estimation, where the goal is to use measured outputs to estimate unknown internal states, the goal of input reconstruction is to use measured outputs to estimate unknown inputs. Although not as well known as the state-estimation problem, input reconstruction has been studied for several decades, and interest continues up to the present time [1–13].

Early research focused on the problem of reconstructing the input given knowledge of the initial state of the system, while more recent techniques have focused on the problem of input reconstruction when the initial state is unknown. The latter problem is more challenging when zeros are present in the system since, for a suitable initial condition and input sequence, the output can be identically zero, thus making it impossible to unambiguously reconstruct the input.

When the initial condition is unknown and zeros are present in the plant, it is, however, possible to generically reconstruct the input asymptotically [7, 11, 12]. The simplest case occurs when the system is minimum phase, that is, all transmission zeros are stable. In this case, the input reconstruction error decays with time [13]. The case of transmission zeros on the unit circle is intractable since the input reconstruction error is persistent. Finally, the case of nonminimum-phase transmission zeros is the most interesting, since the error decays as the reverse system propagates forward, that is, the input-reconstruction estimates are propagated backwards in time [7, 11, 12]. In practice, this means that the ability to reconstruct inputs to a nonminimum-phase system entails a delay in obtaining the input estimates.

This work was supported in part by NASA GSRP grant NNX09AO55H and IRAC grant NNX08AB92A.

A. M. D'Amato and D. S. Bernstein are with the Department of Aerospace Engineering, University of Michigan, Ann Arbor, MI, USA. {amdamato, dsbaero}@umich.edu

In the present paper we propose a new approach to input reconstruction that is based entirely on forward propagation of the input estimate. This approach is especially suitable for harmonic inputs, that is, inputs that consist of sinusoids of different frequencies, and is applicable to plants with arbitrary zeros. Inversion techniques for nonminimum-phase systems are used in [17] for tracking and iterative learning control.

We present two algorithms for forward-propagating input reconstruction. In open-loop forward-propagating input reconstruction, we construct a finite-impulse-response (FIR) transfer function that approximates the left inverse of the plant by minimizing the fit error at the frequencies that are present in the input signal. Although this method is applicable even for nonminimum-phase systems, the drawback is that the input spectrum must be known.

For the case in which the input spectrum is uncertain, we consider a closed-loop forward-propagating input-reconstruction technique, where the error is used to adapt the FIR approximate inverse based on the output residual. The adaptation algorithm uses a surrogate performance variable and a retrospective cost function. This technique is used in retrospective cost adaptive control (RCAC) [14] as well as retrospective cost model refinement. The present paper thus shows that, in addition to being of interest for its own sake, the adaptive forward-propagating input-reconstruction has implications beyond the problem of input reconstruction.

In this paper we first provide a problem formulation for the forward-propagating input reconstruction problem. Next, we develop an open-loop method for input reconstruction in the presence of nonminimum-phase zeros using an asymptotically stable, partial inverse. We demonstrate the open-loop method on several examples. In Section V we introduce an adaptive closed-loop method using residual-based optimization to determine a partial inverse of the system. We then demonstrate the method on several illustrative examples.

II. Problem Formulation

Consider the MIMO discrete-time system

$$x(k+1) = Ax(k) + Bu(k), \tag{1}$$

$$y(k) = Cx(k), \tag{2}$$

where $A \in \mathbb{R}^{n\times n}$ is asymptotically stable, $B \in \mathbb{R}^{n\times m}$, and $C \in \mathbb{R}^{p\times n}$, $x(k) \in \mathbb{R}^n$, $y(k) \in \mathbb{R}^p$, and $u(k) \in \mathbb{R}^m$. Next,

978-1-4577-1094-0/12/$26.00 ©2012 AACC

we define

$$G(\mathbf{q}) \triangleq C(\mathbf{q}I - A)^{-1}B \in \mathbb{R}^{p\times m}(\mathbf{q}), \tag{3}$$

where $\mathbf{q}$ is the forward shift operator and $y(k) = G(\mathbf{q})u(k)$. We assume that $G(\mathbf{q})$ has full normal column rank, which implies that $m = \text{rank } B \leq \text{rank } C = p$.

We assume that $u(k)$ is a harmonic signal with frequencies in the set $\mathbf{\Omega} \triangleq \{\Omega_1, \ldots, \Omega_h\}$, where $0 < \Omega_i < \pi$ rad/sample for all $i = 1, \ldots, h$. Next, let $F(\mathbf{q}) \in \mathbb{R}^{m\times p}(\mathbf{q})$ and define the signals

$$\hat{u}(k) \triangleq F(\mathbf{q})y(k), \tag{4}$$

$$\hat{y}(k) \triangleq G(\mathbf{q})\hat{u}(k), \tag{5}$$

where $\hat{u}(k) \in \mathbb{R}^m$, $\hat{y}(k) \in \mathbb{R}^p$. Furthermore,

$$z(k) \triangleq \hat{y}(k) - y(k), \tag{6}$$

$$\tilde{u}(k) \triangleq \hat{u}(k) - u(k). \tag{7}$$

The goal is to determine $F(\mathbf{q})$ such that $\tilde{u}(k)$ is small. Note that $\tilde{u}(k)$ is unknown, since $u(k)$ is unknown.

III. Open-Loop Forward-Propagating Input Reconstruction

Figure 1 shows the open-loop architecture in which $F(\mathbf{q})$ is cascaded with $G(\mathbf{q})$ to give estimates $\hat{u}(k)$ of $u(k)$. To determine $F(\mathbf{q})$ we consider the strictly proper finite-

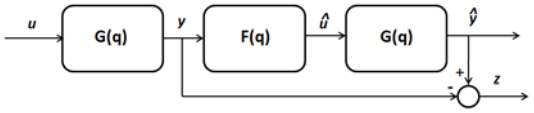

Fig. 1. Open-loop architecture for input reconstruction. In this setup, the performance z, is not used to improve the estimate $\hat{u}$ of u.

impulse-response (FIR) system

$$F(\mathbf{q}) = \sum_{i=1}^{\ell} \mathbf{q}^{-i}\beta_i \in \mathbb{R}^{m\times p}, \tag{8}$$

where $\beta_i \in \mathbb{R}^{m\times p}$, for all $i = 1, \ldots, \ell$. The goal is to determine $\beta_1, \ldots, \beta_\ell$ such that

$$J(\mathbf{\Omega}) \triangleq \sqrt{\text{tr Re}[(\varepsilon^*(\mathbf{\Omega})\varepsilon(\mathbf{\Omega}))]}, \tag{9}$$

is minimized where

$$\varepsilon(\mathbf{\Omega}) = \begin{bmatrix} F(e^{\jmath\Omega_1}) - G^\dagger(e^{\jmath\Omega_1}) & \cdots & F(e^{\jmath\Omega_h}) - G^\dagger(e^{\jmath\Omega_h}) \end{bmatrix}, \tag{10}$$

$(\cdot)^*$ denotes the complex conjugate transpose, and

$$G^\dagger(\mathbf{q}) = [G^{\mathrm{T}}(\mathbf{q})G(\mathbf{q})]^{-1}G^{\mathrm{T}}(\mathbf{q}), \tag{11}$$

which is improper.

To determine $\beta_1, \ldots \beta_\ell$ we choose the frequency set $\bar{\mathbf{\Omega}} = \{\bar{\Omega}_1, \ldots, \bar{\Omega}_l\}$. If $\mathbf{\Omega}$ is known, then we can set $\bar{\mathbf{\Omega}} = \mathbf{\Omega}$. If, however, $\mathbf{\Omega}$ is unknown, then $\bar{\mathbf{\Omega}}$ can be chosen to approximate or cover $\mathbf{\Omega}$. We then minimize $J(\bar{\mathbf{\Omega}})$ with respect to $\beta_1, \ldots, \beta_\ell$. We thus have the linear relation

$$\Psi = \Lambda\Phi, \tag{12}$$

where $\Psi \in \mathbb{R}^{m\times jp}$, $\Lambda \in \mathbb{R}^{m\times lp}$, $\Phi \in \mathbb{R}^{lp\times lp}$,

$$\Psi \triangleq \Big[\text{Re}[G^\dagger(e^{\jmath\bar{\Omega}_1})]\ \text{Im}[G^\dagger(e^{\jmath\bar{\Omega}_1})] \cdots \text{Re}[G^\dagger(e^{\jmath\bar{\Omega}_l})]\ \text{Im}[G^\dagger(e^{\jmath\bar{\Omega}_l})]\Big], \tag{13}$$

$$\Lambda \triangleq \begin{bmatrix} \beta_1 & \cdots & \beta_\ell \end{bmatrix}, \tag{14}$$

and

$$\Phi \triangleq \begin{bmatrix} \text{Re}[e^{-\jmath\bar{\Omega}_1}] & \text{Im}[e^{-\jmath\bar{\Omega}_1}] & \cdots & \text{Re}[e^{-\jmath\bar{\Omega}_l}] & \text{Im}[e^{-\jmath\bar{\Omega}_l}] \\ \vdots & \vdots & \vdots & \vdots & \vdots \\ \text{Re}[e^{-\ell\jmath\bar{\Omega}_1}] & \text{Im}[e^{-\ell\jmath\bar{\Omega}_1}] & \cdots & \text{Re}[e^{-\ell\jmath\bar{\Omega}_l}] & \text{Im}[e^{-\ell\jmath\bar{\Omega}_l}] \end{bmatrix}. \tag{15}$$

The least-squares solution of (12) is given by

$$\Lambda_{\text{opt}} = \Psi\Phi^{\mathrm{T}}(\Phi\Phi^{\mathrm{T}})^{-1}, \tag{16}$$

which minimizes $J(\bar{\mathbf{\Omega}})$. Note that if $G(\mathbf{q})$ is nonminimum phase, then $G^\dagger(\mathbf{q})$ is unstable. However, the poles of $F(\mathbf{q})$ are located at the origin, and therefore $F(\mathbf{q})$ is asymptotically stable.

IV. Open-loop examples

Consider the asymptotically stable, nonminimum-phase plant $G(\mathbf{q}) = \frac{(\mathbf{q}-0.4)(\mathbf{q}-1.5)}{(\mathbf{q}-0.5\pm0.5\jmath)(\mathbf{q}-0.7)}$. We demonstrate input reconstruction for an unknown three-tone signal.

In the first example, we assume that the selected fit frequencies $\bar{\mathbf{\Omega}}$ coincide with the input frequencies $\mathbf{\Omega}$. In the second example, we assume that $\mathbf{\Omega}$ is a subset of $\bar{\mathbf{\Omega}}$, and, finally, $\mathbf{\Omega}$ is not a subset of $\bar{\mathbf{\Omega}}$.

In each case the unknown input is $u(k) = 0.01\sin(\Omega_1 k) + 0.63\sin(\Omega_2 k) + 1.3\sin(\Omega_3 k)$, where $\Omega_1 = 0.5$, $\Omega_2 = 0.7$, and $\Omega_3 = 0.9$ rad/sample.

Example 4.1: (SISO NMP, $\mathbf{\Omega} = \bar{\mathbf{\Omega}}$) Figure 2 is the frequency response comparison of F and $G^\dagger$, where the red vertical lines denote the frequencies $\bar{\Omega}_i$. At the frequencies $\bar{\Omega}_i$ the fit error is small, namely, $\|\varepsilon(\mathbf{\Omega})\| = 9.66 \times 10^{-12}$. Figure 3 compares the input $u(k)$ and the estimated input

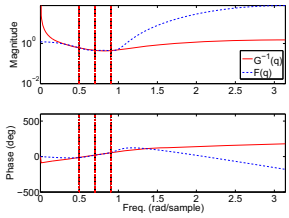

Fig. 2. Frequency response comparison of F and $G^\dagger$, where the red vertical lines denote the frequencies $\bar{\Omega}_i$. In this example, $\bar{\mathbf{\Omega}} = \mathbf{\Omega}$.

$\hat{u}(k)$. The peak of the transient not shown is ± 10. Figure 4 shows the residual plots of $\tilde{u}(k)$ and $z(k)$.

Example 4.2: (SISO NMP, $\mathbf{\Omega}$ is not a subset of $\bar{\mathbf{\Omega}}$) For this example we choose $\bar{\Omega}_1 = 0.2$, $\bar{\Omega}_2 = 0.57$, $\bar{\Omega}_3 = 0.6$,

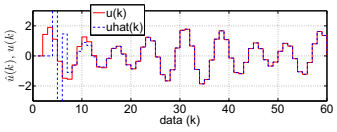

Fig. 3. Comparison between $\hat{u}(k)$ and $u(k)$. After a transient whose peak excursion is approximately ± 10, $\tilde{u}(k)$ is small.

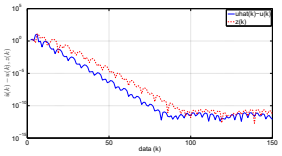

Fig. 4. Residuals $\tilde{u}(k)$ and $z(k)$ show that both the input reconstruction error and output residual become small.

$\bar{\Omega}_4 = 0.76$, $\bar{\Omega}_5 = 0.95$, and $\bar{\Omega}_6 = 1.1$. Figure 5 is the frequency response comparison of F and $G^\dagger$, where the red vertical lines denote the frequencies $\bar{\mathbf{\Omega}}$. The fit error is $\|\varepsilon(\mathbf{\Omega})\| = 0.14$. Next we choose $\bar{\Omega}_1 = 0.01$, $\bar{\Omega}_2 = 0.2$, $\bar{\Omega}_3 = 0.75$, $\bar{\Omega}_4 = 0.9$, $\bar{\Omega}_5 = 1.5$. Figure 6 compares the input

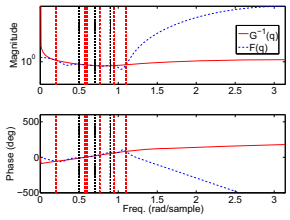

Fig. 5. Frequency response comparison of F and $G^\dagger$, where the dashed vertical lines denote the frequencies $\bar{\mathbf{\Omega}}$, and the dotted vertical lines are the frequencies $\mathbf{\Omega}$.

$u(k)$ and the estimated input $\hat{u}(k)$. The peak of the transient not shown is approximately $\pm 5 \times 10^3$. Figure 7 shows the

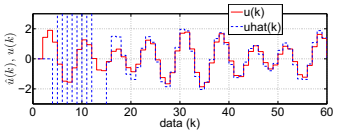

Fig. 6. Comparison between $\hat{u}(k)$ and $u(k)$. After a transient whose peak excursion is approximately $\pm 5 \times 10^3$, $\tilde{u}(k)$ is small.

residual plots of $\tilde{u}(k)$ and $\tilde{y}(k)$.

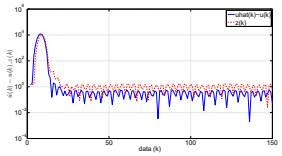

Fig. 7. Residuals $\tilde{u}(k)$ and $z(k)$ show that both the input reconstruction error and output residual become small.

V. Closed-Loop Forward-Propagating Input Reconstruction

We now consider the case where the output residual $z(k)$ is used to adaptively tune the parameters of $F(\mathbf{q})$ as in Figure 8. We start by letting $\hat{u}(k)$ be the output of the strictly proper

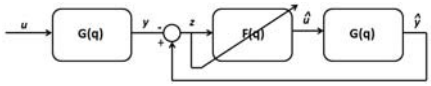

Fig. 8. Adaptive architecture for input reconstruction.

adaptive feedback system of order ℓ, given by

$$\hat{u}(k) = \sum_{i=1}^{\ell} M_i(k)\hat{u}(k-i) + \sum_{i=1}^{\ell} N_i(k)z(k-i), \qquad (17)$$

where, for all $i = 1, \ldots, \ell$, $M_i(k) \in \mathbb{R}^{m\times m}$ and $N_i(k) \in \mathbb{R}^{m\times p}$. Note that we now take $z(k)$ to be the input the input to $F(\mathbf{q})$. The goal is to update $M_i(k)$ and $N_i(k)$ using the measured output error $z(k)$. Note that the coefficients of $F(\mathbf{q})$ are $M_i(k)$ and $N_i(k)$.

A. Input Reconstruction using a Retrospective Surrogate Cost

For $i \geq 1$, define the Markov parameter H_i of (A, B, C) given by

$$H_i \triangleq CA^{i-1}B. \qquad (18)$$

For example, $H_1 = CB$ and $H_2 = CAB$. Let r be a positive integer. Then, for all $k \geq r$,

$$\hat{x}(k) = A^r\hat{x}(k-r) + \sum_{i=1}^{r} A^{i-1}B\hat{u}(k-i), \qquad (19)$$

and thus

$$z(k) = CA^r\hat{x}(k-r) - y(k) + \bar{H}\hat{\bar{U}}(k-1), \qquad (20)$$

where

$$\bar{H} \triangleq \begin{bmatrix} H_1 & \cdots & H_r \end{bmatrix} \in \mathbb{R}^{p\times rm}$$

and

$$\bar{U}(k-1) \triangleq [\hat{u}^{\mathrm{T}}(k-1) \quad \cdots \quad \hat{u}^{\mathrm{T}}(k-r)]^{\mathrm{T}}.$$

Next, we rearrange the columns of $\bar{H}$ and the components of $\hat{\bar{U}}(k-1)$ and partition the resulting matrix and vector so that

$$\bar{H}\hat{\bar{U}}(k-1) = \mathcal{H}'\hat{U}'(k-1) + \mathcal{H}\hat{U}(k-1), \qquad (21)$$

where $\mathcal{H}' \in \mathbb{R}^{p\times m(r-\rho)}$, $\mathcal{H} \in \mathbb{R}^{p\times m\rho}$, $\hat{U}'(k-1) \in \mathbb{R}^{m(r-\rho)}$, and $\hat{U}(k-1) \in \mathbb{R}^{m\rho}$. Then, we can rewrite (20) as

$$z(k) = \mathcal{S}(k) + \mathcal{H}\hat{U}(k-1), \qquad (22)$$

where

$$\mathcal{S}(k) \triangleq CA^r\hat{x}(k-r) - y(k) + \mathcal{H}'\hat{U}'(k-1). \qquad (23)$$

Next, for $j = 1, \ldots, s$, we rewrite (22) with a delay of k_j time steps, where $0 \leq k_1 \leq k_2 \leq \cdots \leq k_s$, in the form

$$z(k-k_j) = \mathcal{S}_j(k-k_j) + \mathcal{H}_j \hat{U}_j(k-k_j-1), \tag{24}$$

where (23) becomes

$$\mathcal{S}_j(k-k_j) \triangleq CA^r x(k-k_j-r) - y(k-k_j) + \mathcal{H}_j' \hat{U}_j'(k-k_j-1)$$

and (21) becomes

$$\bar{H}\hat{\tilde{U}}(k-k_j-1) = \mathcal{H}_j' \hat{U}_j'(k-k_j-1) + \mathcal{H}_j \hat{U}_j(k-k_j-1), \tag{25}$$

where $\mathcal{H}_j' \in \mathbb{R}^{p \times m(r-\rho_j)}$, $\mathcal{H}_j \in \mathbb{R}^{p \times m\rho_j}$, $\hat{U}_j'(k-k_j-1) \in \mathbb{R}^{m(r-\rho_j)}$, and $\hat{U}_j(k-k_j-1) \in \mathbb{R}^{m\rho_j}$. Now, by stacking $z(k-k_1), \ldots, z(k-k_s)$, we define the *extended performance*

$$Z(k) \triangleq \begin{bmatrix} z^{\mathrm{T}}(k-k_1) & \cdots & z^{\mathrm{T}}(k-k_s) \end{bmatrix}^{\mathrm{T}} \in \mathbb{R}^{sp}. \tag{26}$$

Therefore,

$$Z(k) \triangleq \tilde{\mathcal{S}}(k) + \tilde{\mathcal{H}}\hat{\tilde{U}}(k-1), \tag{27}$$

where

$$\tilde{\mathcal{S}}(k) \triangleq \begin{bmatrix} \mathcal{S}_1{}^{\mathrm{T}}(k-k_1) & \cdots & \mathcal{S}_s{}^{\mathrm{T}}(k-k_s) \end{bmatrix}^{\mathrm{T}} \in \mathbb{R}^{sp}, \tag{28}$$

$\hat{\tilde{U}}(k-1)$ has the form

$$\hat{\tilde{U}}(k-1) \triangleq \begin{bmatrix} \hat{u}^{\mathrm{T}}(k-q_1) & \cdots & \hat{u}^{\mathrm{T}}(k-q_g) \end{bmatrix}^{\mathrm{T}} \in \mathbb{R}^{mg}, \tag{29}$$

where, for $i = 1, \ldots, g$, $k_1 + 1 \leq q_i \leq k_s + 1$, and $\tilde{\mathcal{H}} \in \mathbb{R}^{sp \times mg}$ is constructed according to the structure of $\hat{\tilde{U}}(k-1)$. The vector $\hat{\tilde{U}}(k-1)$ is formed by stacking $\hat{U}_1(k-k_1-1), \ldots, \hat{U}_s(k-k_s-1)$ and removing copies of repeated components.

Next, we define the *surrogate performance*

$$\hat{z}_j(k-k_j) \triangleq \mathcal{S}_j(k-k_j) + \mathcal{H}_j U_j^*(k-k_j-1), \tag{30}$$

where the past controls $\hat{U}_j(k-k_j-1)$ in (24) are replaced by the surrogate controls $U_j^*(k-k_j-1)$. In analogy with (26), the *extended surrogate performance* for (30) is defined as

$$\hat{Z}(k) \triangleq \begin{bmatrix} \hat{z}_j^{\mathrm{T}}(k-k_1) & \cdots & \hat{z}_j^{\mathrm{T}}(k-k_s) \end{bmatrix}^{\mathrm{T}} \in \mathbb{R}^{sp} \tag{31}$$

and thus is given by

$$\hat{Z}(k) = \tilde{\mathcal{S}}(k) + \tilde{\mathcal{H}}\tilde{U}^*(k-1), \tag{32}$$

where the components of $\tilde{U}^*(k-1) \in \mathbb{R}^{l_{\tilde{U}}}$ are the components of $U_1^*(k-k_1-1), \ldots, \hat{U}_s^*(k-k_s-1)$ ordered in the same way as the components of $\hat{\tilde{U}}(k-1)$. Subtracting (27) from (32) yields

$$\hat{Z}(k) = Z(k) - \tilde{\mathcal{H}}\hat{\tilde{U}}(k-1) + \tilde{\mathcal{H}}\tilde{U}^*(k-1). \tag{33}$$

Finally, we define the *retrospective cost function*

$$\bar{J}(\tilde{U}^*(k-1), k) \triangleq \hat{Z}^{\mathrm{T}}(k) R(k) \hat{Z}(k) + \eta(k) \tilde{U}^{*\mathrm{T}}(k-1) \tilde{U}^*(k-1), \tag{34}$$

where $R(k) \in \mathbb{R}^{ps \times ps}$ is a positive-definite performance weighting and $\eta(k) = \eta_0 z(k)^{\mathrm{T}} z(k)$. η_0 is chosen to guarantee the boundedness of $\hat{\tilde{U}}(k)$.

The goal is to determine refined controls $\hat{\tilde{U}}(k-1)$ that would have provided better performance than the controls $U(k)$ that were applied to the system. The refined control values $\tilde{U}^*(k-1)$ are subsequently used to update the controller. Substituting (33) into (34) yields

$$\bar{J}(\tilde{U}^*(k-1), k) = \tilde{U}^*(k-1)^{\mathrm{T}} \mathcal{A}(k) \tilde{U}^*(k-1) + \tilde{U}^{*\mathrm{T}} \mathcal{B}^{\mathrm{T}}(k)(k-1) + \mathcal{C}(k), \tag{35}$$

where

$$\mathcal{A}(k) \triangleq \tilde{\mathcal{H}}^{\mathrm{T}} R(k) \tilde{\mathcal{H}} + \eta(k) I_{mg}, \tag{36}$$

$$\mathcal{B}(k) \triangleq 2\tilde{\mathcal{H}}^{\mathrm{T}} R(k) [Z(k) - \tilde{\mathcal{H}}\hat{\tilde{U}}(k-1)], \tag{37}$$

$$\mathcal{C}(k) \triangleq Z^{\mathrm{T}}(k) R(k) Z(k) - 2Z^{\mathrm{T}}(k) R(k) \tilde{\mathcal{H}}\hat{\tilde{U}}(k-1) + \hat{\tilde{U}}^{\mathrm{T}}(k-1) \tilde{\mathcal{H}}^{\mathrm{T}} R(k) \tilde{\mathcal{H}} \hat{\tilde{U}}(k-1). \tag{38}$$

If either $\tilde{\mathcal{H}}$ has full column rank or $\eta(k) > 0$, then $\mathcal{A}(k)$ is positive definite. In this case, $\bar{J}(\hat{\tilde{U}}(k-1), k)$ has the unique global minimizer

$$\tilde{U}^*(k-1) = -\frac{1}{2} \mathcal{A}^{-1}(k) \mathcal{B}(k). \tag{39}$$

B. Adaptive Feedback Update

The control (17) can be expressed as

$$\hat{u}(k) = \theta(k) \phi(k-1), \tag{40}$$

where

$$\theta(k) \triangleq [M_1(k) \ \cdots \ M_\ell(k) \ N_1(k) \ \cdots \ N_\ell(k)] \in \mathbb{R}^{m \times \ell(m+p)} \tag{41}$$

and

$$\phi(k-1) \triangleq [\hat{u}^{\mathrm{T}}(k-1) \ \cdots \ \hat{u}^{\mathrm{T}}(k-\ell) \ z^{\mathrm{T}}(k-1) \ \cdots \ z^{\mathrm{T}}(k-\ell) \ ]^{\mathrm{T}} \in \mathbb{R}^{\ell(m+p)}. \tag{42, 43}$$

Next, we define the cumulative cost function

$$J_{\mathrm{R}}(\theta(k)) \triangleq \sum_{i=g+1}^{k} \lambda^{k-i} \| \phi^{\mathrm{T}}(i-g-1)\theta^{\mathrm{T}}(k) - u^{*\mathrm{T}}(i-g) \|^2 + \lambda^k (\theta(k) - \theta(0))^{\mathrm{T}} P^{-1}(0) (\theta(k) - \theta(0)), \tag{44}$$

where $\| \cdot \|$ is the Euclidean norm, and $\lambda(k) \in (0, 1]$ is the forgetting factor. Minimizing (44) yields

$$\theta^{\mathrm{T}}(k) \triangleq \theta^{\mathrm{T}}(k-1) + \alpha(k) P(k-1) \phi(k-g-1) \cdot [\phi^{\mathrm{T}}(k-g-1) P(k-1) \phi(k-g-1) + \lambda(k)]^{-1} \cdot [\phi^{\mathrm{T}}(k-g-1) \theta^{\mathrm{T}}(k-1) - \hat{u}^{\mathrm{T}}(k-g)], \tag{45}$$

The error covariance is updated by

$$\begin{aligned} P(k) \triangleq\ & (1-\alpha(k))P(k-1) + \alpha(k)\lambda^{-1}(k)P(k-1) \\ & - \alpha(k)\lambda^{-1}(k)P(k-1)\phi(k-g-1) \\ & \cdot [\phi^{\mathrm{T}}(k-g-1)P(k-1)\phi(k-g-1) + \lambda(k)]^{-1} \\ & \cdot \phi^{\mathrm{T}}(k-g-1)P(k-1). \end{aligned} \tag{46}$$

We initialize the error covariance matrix as $P(0) = \gamma I$, where $\gamma > 0$.

C. Approximating $G(\mathbf{q})$ with $\tilde{\mathcal{H}}$

Let $G_{\mathrm{FIR}}(\mathbf{q})$ be an FIR transfer function whose numerator coefficients are the Markov parameters of G_{zu} that appear in $\tilde{\mathcal{H}}$. The retrospective surrogate cost approximates the inputs $u^*(k)$, using an FIR approximation of the plant $G(\mathbf{q})$. We analyze the robustness of the algorithm to error in $G_{\mathrm{FIR}}(\mathbf{q})$.

Assume that the system is turned on at $k = 1$ and allowed to reach harmonic steady state, which occurs approximately at $k_0 > k$. Then for $0 \leq k_i < k_0$, $\alpha(k_i) = 0$, and $\alpha(k_0) = 1$. Furthermore, $\alpha(k_0 + 1) = 0$, where $\alpha(k) = 1$, once the system has again reached harmonic steady state.

Assume that $\tilde{\mathcal{H}}$ has full column rank, $\eta(k) \to 0$ as $z(k) \to 0$, $R(k) = I$, $Z(k)$ is in the range of $\tilde{\mathcal{H}}$, and let $\hat{\tilde{U}}(k-1)$ be given by (39). Furthermore, assume that $u(k) - \hat{u}(k) \to 0$ as $k \to \infty$ and

$$\left| 1 - \frac{G(e^{\jmath\Omega})}{G_{\mathrm{FIR}}(e^{\jmath\Omega})} \right| < 1. \tag{47}$$

Then $z(k) \to 0$ as $k \to \infty$. To show this, in harmonic steady state we have

$$z_\nu = -G(e^{\jmath\Theta})u + G(e^{\jmath\Theta})u^*_\nu + G(e^{\jmath\Theta})g_\nu, \tag{48}$$

where z_ν, u^*_ν, g_ν are phasors, and $g_\nu \triangleq u_\nu - \hat{u}_\nu$. In view of the assumption that $\hat{u}(k) - u^*(k) \to 0$ as $k \to \infty$, we assume that g_ν is negligible and omitted for simplicity.

Next, the retrospective cost in harmonic steady state is,

$$\hat{z}_\nu \triangleq z_{\nu-1} - G_{\mathrm{FIR}}(e^{\jmath\Theta})u^*_{\nu-1} + G_{\mathrm{FIR}}(e^{\jmath\Theta})u^*_\nu, \tag{49}$$

$$\begin{aligned} \hat{z}_\nu =\ & -G(e^{\jmath\Theta})u + G(e^{\jmath\Theta})u^*_{\nu-1} - G_{\mathrm{FIR}}(e^{\jmath\Theta})u^*_{\nu-1} \\ & + G_{\mathrm{FIR}}(e^{\jmath\Theta})u^*_\nu, \end{aligned} \tag{50}$$

$$\begin{aligned} \hat{z}_\nu =\ & [G(e^{\jmath\Theta}) - G_{\mathrm{FIR}}(e^{\jmath\Theta})]u^*_{\nu-1} \\ & + G_{\mathrm{FIR}}(e^{\jmath\Theta})u^*_\nu - G(e^{\jmath\Theta})u. \end{aligned} \tag{51}$$

Solving (51) for u^*_ν yields,

$$\begin{aligned} u^*_\nu =\ & G^{-1}_{\mathrm{FIR}}(e^{\jmath\Theta})[\hat{z}_\nu + G(e^{\jmath\Theta})u \\ & - [G(e^{\jmath\Theta}) - G_{\mathrm{FIR}}(e^{\jmath\Theta})]u^*_{\nu-1}]. \end{aligned} \tag{52}$$

Substituting (52) into (48) yields,

$$\begin{aligned} z_\nu =\ & [1 - G(e^{\jmath\Theta})G^{-1}_{\mathrm{FIR}}(e^{\jmath\Theta})][-G(e^{\jmath\Theta})u + G(e^{\jmath\Theta})u^*_{\nu-1}] \\ & + G(e^{\jmath\Theta})G^{-1}_{\mathrm{FIR}}(e^{\jmath\Theta})\hat{z}_\nu. \end{aligned} \tag{53}$$

Using this process we write z_ν in terms of u^*_0 as

$$\begin{aligned} z_\nu =\ & [1 - G(e^{\jmath\Theta})G^{-1}_{\mathrm{FIR}}(e^{\jmath\Theta})]^\nu [-G(e^{\jmath\Theta})u + G(e^{\jmath\Theta})u^*_0] \\ & + \sum_{i=0}^{\nu} [1 - G(e^{\jmath\Theta})G^{-1}_{\mathrm{FIR}}(e^{\jmath\Theta})]^i [G(e^{\jmath\Theta})G^{-1}_{\mathrm{FIR}}(e^{\jmath\Theta})]\hat{z}_{\nu-i}. \end{aligned} \tag{54}$$

It follows from (54) that

$$\begin{aligned} |z_\nu| \leq\ & \left|1 - G(e^{\jmath\Theta})G^{-1}_{\mathrm{FIR}}(e^{\jmath\Theta})\right|^\nu \left|-G(e^{\jmath\Theta})u + G(e^{\jmath\Theta})u^*_0\right| \\ & + \left|\sum_{i=0}^{\nu} [1 - G(e^{\jmath\Theta})G^{-1}_{\mathrm{FIR}}(e^{\jmath\Theta})]^i [G(e^{\jmath\Theta})G^{-1}_{\mathrm{FIR}}(e^{\jmath\Theta})]\hat{z}_{\nu-i}\right|. \end{aligned} \tag{55}$$

Therefore, since $\left|1 - \frac{G(e^{\jmath\Theta})}{G_{\mathrm{FIR}}(e^{\jmath\Theta})}\right| < 1$, it follows that $\left|1 - \frac{G(e^{\jmath\Theta})}{G_{\mathrm{FIR}}(e^{\jmath\Theta})}\right|^\nu \to 0$ as $\nu \to \infty$, then $|z_\nu| \to 0$ as $\nu \to \infty$.

Condition (47) has a simple geometric interpretation, namely, $G_{\mathrm{FIR}}(e^{\jmath\Omega})$ must lie in a half plane that contains $G(e^{\jmath\Omega})$ and whose boundary is perpendicular to a line drawn from the origin to $|G(e^{\jmath\Omega})|$ and passes through $\frac{1}{2}|G(e^{\jmath\Omega})|$. Figure 9 illustrates the region of admissible $G_{\mathrm{FIR}}(e^{\jmath\Omega})$ for a given $|G(e^{\jmath\Omega})|$ and frequency Ω.

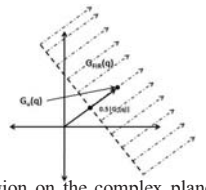

Fig. 9. The dashed region on the complex plane illustrates the region of admissible $G_{\mathrm{FIR}}(e^{\jmath\Omega})$ for a given $|G(e^{\jmath\Omega})|$ and frequency Ω as determined by (47). The admissible region is a half plane.

The above analysis is based on the assumption that the state of the system reaches harmonic steady state after each period of adaptation. This assumption is an approximation invoked to facilitate the analysis. In fact, RCAC adapts at each step, and thus the state does not reach harmonic steady state. The examples in the next section show that this condition is sufficient but not necessary, and thus provides a conservative estimate of the allowable uncertainty that can be tolerated in the FIR approximation error.

VI. Adaptive Examples

We now re-consider the same plant and unknown input as in Section IV. We now apply the adaptive algorithm in place of the open-loop input reconstruction technique. For all of the following examples we choose the RCAC parameters $\ell = 10$, $\eta_0 = 0.01$, and $P(0) = 1$.

Example 6.1: (SISO NMP, $\tilde{\mathcal{H}} = H_1$) In the first example we choose $\tilde{\mathcal{H}} = H_1$. Figure 10 compares the frequency response of $G(\mathbf{q})$ and $G_{\mathrm{FIR}}(\mathbf{q}) = \frac{H_1}{\mathbf{q}}$. Note from the

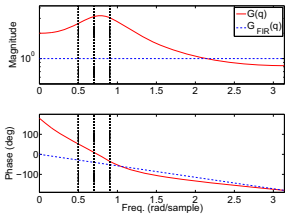

Fig. 10. Frequency response comparison of G and G_{FIR}, where the red vertical lines denote the frequencies Ω_i.

phase comparison that the phase error at frequency Ω_1 is approaching 90 degrees. Figure 11 compares the effect of the large phase error, where a large transient is experienced

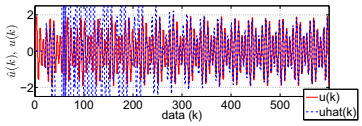

Fig. 11. Comparison between $\hat{u}(k)$ and $u(k)$. After a transient whose peak excursion is approximately $\pm 4 \times 10^5$, $\tilde{u}(k)$ is small.

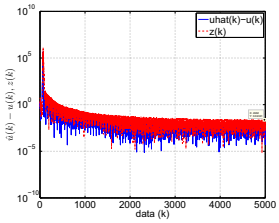

Fig. 12. Residuals $\hat{u}(k) - u(k)$ and $z(k)$ show that both the input reconstruction error and the output residual become small.

before settling. Figure 12 compares the residual $\hat{u}(k) - u(k)$ and $z(k)$. We note that the performance does not reach a lower bound as in the open-loop case, but continues to decrease.

Example 6.2: (SISO NMP, $\tilde{\mathcal{H}} = [H_3 \ H_2 \ H_1]^{\mathrm{T}}$) In the first example we choose $\tilde{\mathcal{H}} = [H_3 \ H_2 \ H_1]^{\mathrm{T}}$. Figure 13 compares the frequency response of $G(\mathbf{q})$ and $G_{\mathrm{FIR}}(\mathbf{q}) = \frac{H_1\mathbf{q}^2 + H_2\mathbf{q} + H_3}{\mathbf{q}^3}$. Note from the phase comparison that the

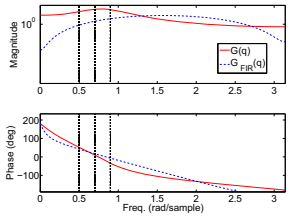

Fig. 13. Frequency response comparison of G and G_{FIR}, where the red vertical lines denote the frequencies Ω_i.

phase error is smaller than the previous example.

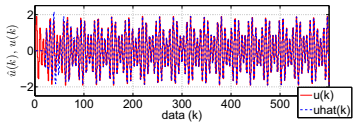

Fig. 14. Comparison between $\hat{u}(k)$ and $u(k)$. Note that in this case $\tilde{u}(k)$ is small, with no transient.

Figure 14 compares the improved transient performance over the previous example since G_{FIR} is a better approximation of G at the relevant frequencies.

Figure 15 shows the residual $\hat{u}(k) - u(k)$ and $z(k)$.

VII. Conclusions

In this paper we presented two methods for forward-propagating input reconstruction for nonminimum-phase systems. First we developed an open-loop method, which uses

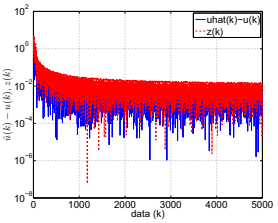

Fig. 15. Residuals $\hat{u}(k) - u(k)$ and $z(k)$ show that both the input reconstruction error and the output residual become small.

a finite impulse response (FIR) model to approximate the inverse of the system at a finite number of frequencies. This FIR model was then used with the measured system output to estimate the system input. Next, we presented a closed-loop method, which uses the output residual to adaptively tune the coefficients of an infinite impulse response transfer function to estimate the system input. The closed-loop method is able to minimize the error $\tilde{u}(k)$ despite inaccuracy in the system estimate at the frequencies of the unknown input.

Future research will focus on the effect of sensor noise on the accuracy of the input reconstruction. Finally, the ability to adaptively estimate the phase shift of the transfer function at the input frequency as well as the phase of the input may have applications to the area of phase and frequency estimation [15, 16].

References

[1] L. M. Silverman, Inversion of multivariable linear systems. IEEE Trans. Autom. Control AC-14(3), 270-276 (1969).

[2] M. K. Sain, J.L. Massey, Invertibility of linear time-invariant dynamical systems. IEEE Trans. Autom. Control AC-14(2), 141-149 (1969).

[3] A. S. Willsky, On the invertibility of linear systems. IEEE Trans. Autom. Control AC-19(3), 272-274 (1974).

[4] P. J. Moylan, Stable inversion of linear systems. IEEE Trans. Autom. Control 22(1), 74-78 (1977).

[5] M. Hou, R.J. Patton, Input observability and input reconstruction. Automatica 34(6), 789-794 (1998).

[6] M. Corless, J. Tu, State and input estimation for a class of uncertain systems. Automatica 34(6), 757-764 (1998).

[7] G. Marro, D. Prattichizzo, E. Zattoni, Convolution profiles for right-inversion of multivariable nonminimum phase discrete-time systems. Automatica 38(10), 1695-1703 (2002).

[8] Y. Xiong, M. Saif, Unknown disturbance inputs estimation based on a state functional observer design. Automatica 39, 1389-1398 (2003).

[9] T. Floquet, J.-P. Barbot, State and unknown input estimation for linear discrete-time systems. Automatica 42, 1883-1889 (2006).

[10] H. Palanthandalam-Madapusi and D. S. Bernstein, "A Subspace Algorithm for Simultaneous Identification and Input Reconstruction," *Int. J. Adaptive Contr. Sig. Proc.*, Vol. 23, pp. 1053–1069, 2009.

[11] G. Marro, E. Zattoni, Unknown-state, unknown-input reconstruction in discrete-time nonminimum-phase systems: geometric methods. Automatica 46(5) (2010).

[12] E. Zattoni, G. Marro, and D. S. Bernstein, "A Markov-parameter-based Method for Online Reconstruction of Unknown State and Input in Discrete-Time Systems," *Proc. Conf. Dec. Contr.*, pp. 6022–6027, Atlanta, GA, December 2010.

[13] S. Kirtikar, H. Palanthandalam-Madapusi, E. Zattoni, and D. S. Bernstein, "l-Delay Input and Initial-State Reconstruction for Discrete- Time Linear Systems," Circ. Sys. Sig. Processing, Vol. 30, pp. 233- 262, 2011.

[14] A. M. D'Amato, E. D. Sumer, and D. S. Bernstein, "Frequency-Domain Stability Analysis of Retrospective-Cost Adaptive Control for Systems with Unknown Nonminimum-Phase Zeros," *Proc. Conf. Dec. Contr.*, Orlando, FL, December 2011.

[15] B. G. Quinn, E. J. Hannan, *The Estimation and Tracking of Frequency*, Cambridge University Press, 2001.

[16] T. M. Schmidl, D. C. Cox "Robust frequency and timing synchronization for OFDM," *IEEE Trans. on Communications*, Vol. 45 (12), pp. 1613–1621, 1997.

[17] J. Ghosh, B. Paden, "Iterative Learning Control for Nonlinear Nonminimum Phase Plants," *Trans. ASME,* Vol. 123, pp. 21–30, 2001.